

Measurements of relative angular distributions for the ${}^2\text{H}(\gamma, n)\text{H}$ reaction below 18 MeV

K. E. Stephenson,* R. J. Holt, R. D. McKeown,[†] and J. R. Specht
 Physics Division, Argonne National Laboratory, Argonne, Illinois 60439

(Received 24 February 1987)

High-accuracy angular distribution measurements relative to that at 90° were performed for the ${}^2\text{H}(\gamma, n)\text{H}$ reaction throughout the energy range of 4–18 MeV and for reaction angles of 45° , 135° , and 155° . The results indicate a significant departure from existing theoretical calculations below a photon energy of 10 MeV.

I. INTRODUCTION

Recent studies of the ${}^2\text{H}(\gamma, n)\text{H}$ reaction¹ and the inverse process² have indicated that the reaction mechanism or the meson-exchange current corrections are not fully understood even at low photon energies. As a further test of our understanding of this simple nuclear reaction, high-accuracy measurements of the angular distribution have been performed. It has long been recognized³ that high-accuracy angular distribution measurements of deuteron photodisintegration are necessary as an important test of the multipole decomposition of the electromagnetic excitation. For example, it is now well established⁴ that the cross section for photodisintegration of the deuteron near a reaction angle of 0° or 180° is sensitive⁵ to spin-orbit components of the interaction, while that near 90° is dependent primarily upon the absorption of electric dipole photons. At the intermediate angles there is enhanced sensitivity to electric quadrupole excitation and an accurate measurement of the angular distribution would provide an important constraint on the multipole character of this simplest nuclear reaction. The present work reports on relative angular distribution measurements of unprecedented accuracy for the ${}^2\text{H}(\gamma, n)\text{H}$ reaction.

The primary obstacles to performing high accuracy photoneutron measurements have been the lack of an accurate means to calibrate the efficiency and solid angle of the detectors and minimize multiple scattering effects with the use of thin targets. In the present work, we have minimized these systematic errors by (i) performing measurements relative to the cross section at 90° , (ii) the use of a multidirectional electron beam handling system which permits a simple calibration of the solid angle of the detectors, (iii) measurement of the energy dependence of the neutron efficiency with the use of a well-known fission reaction, and (iv) minimizing neutron multiple scattering in the target with the use of the thinnest targets heretofore reported.

II. EXPERIMENTAL METHOD

The experiment was performed with the novel multidirectional beam transport system at the Argonne high-current electron linac. A schematic diagram of the experimental setup is shown in Fig. 1. The beam transport sys-

tem permitted the electrons to approach the target from one of three different angles which are 90° with respect to one another and form a plane which is perpendicular to the usual reaction plane. These three different electron beam directions are labeled *A*, *B*, and *C* in Fig. 1. When the electron beam approaches from direction *A* the photoneutron reaction angles of 90° , 135° , and 155° are accessible, from direction *B* the angles 45° and 90° are possible. In principle, a reaction angle of 25° is also accessible when the beam approaches from direction *B*, but the copious flux of γ rays from the Al beam stop and bremsstrahlung radiator rendered a measurement at this angle to be impractical.

In summary, the ratios of the cross sections at 45° , 135° , and 155° to that at 90° were measured. The photoneutrons from the target were detected in two plastic scintillators of dimension $10\text{ cm} \times 20\text{ cm} \times 5\text{ cm}$ thick. The detector located at 90° was held fixed while the other detector was free to move to the other positions.

Typical time-of-flight spectra are given in Fig. 2 for an electron energy of 19.0 MeV. The targets consist of rectangular samples of C^2H_2 and equal thicknesses of CH_2 for the background measurements. The normalized background is also shown in Fig. 2 and we note the excellent signal-to-background ratios. The spectrum at 155° is somewhat more compressed owing to a shorter neutron flight path of only 12.8 m rather than 20 m for the other detectors.

The relative efficiencies and solid angles of the detectors can be calibrated when the electron beam is directed

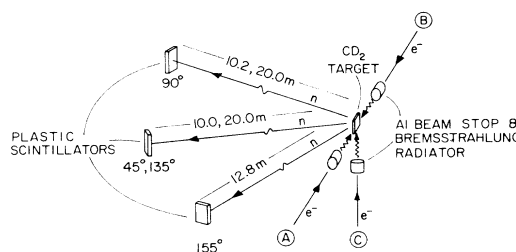


FIG. 1. Schematic diagram of experimental setup. The electron beam can approach the target from three different directions labeled *A*, *B*, and *C* in the illustration.

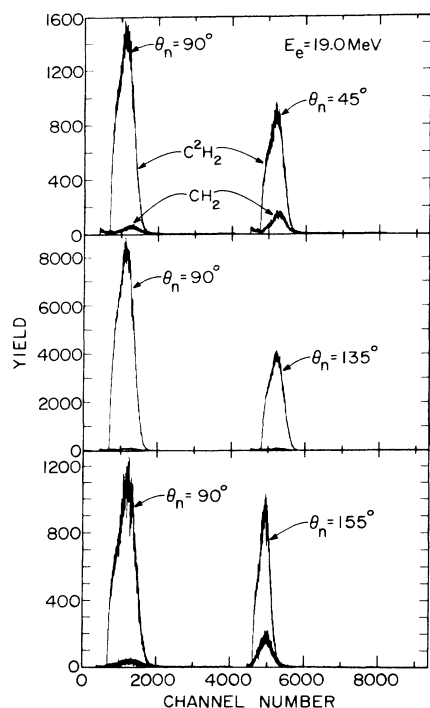


FIG. 2. Raw time-of-flight spectra for the ${}^2\text{H}(\gamma, n)\text{H}$ reaction for $E_e = 19.0$ MeV. Results for both C^2H_2 and CH_2 samples are shown.

to the target from position C. It is this last feature which ensured a high-accuracy measurement of the relative angular distributions. From this angle the detectors, including the collimators, are illuminated uniformly from the target position and the relative solid angle of the two detector systems can be determined. As an indication of the relative solid angles of the two detectors and the accuracy of this determination, a typical measured ratio when the electron beam is directed to the target from position C is given in Fig. 3. It is noted that the relative product of the solid angle and efficiency of the two detectors is very close to unity as expected. The systematic error associated with the relative solid angle and efficiency of the detector system is thus rendered negligible in comparison with other sources of error to be discussed later.

The neutron energies were measured with the time-of-flight method and the photon energies were determined uniquely from the neutron energy. Since a thick bremsstrahlung radiator was used to generate the photons, the analysis was performed in a manner so that no correction was necessary for the bremsstrahlung shape. The ratio of the cross sections at the two angles was determined for a given photon energy, and thus, the bremsstrahlung shape cancelled out of this ratio. However, the photoneutron energies are somewhat different for the two angles for a fixed incident photon energy and it is necessary to provide a small correction based on the energy dependence of the

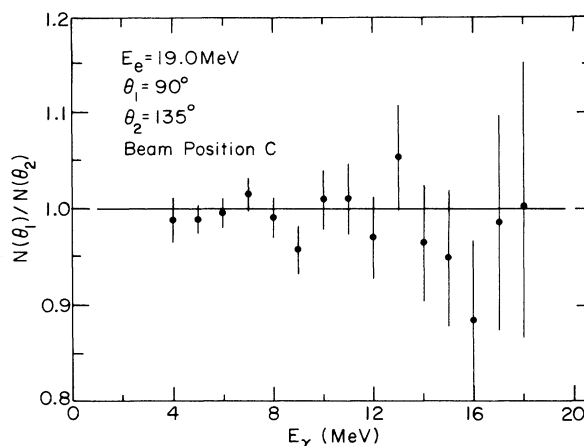


FIG. 3. Typical ratio of photoneutron yields as a function of photon energy. The ratio is the yield at 90° compared with that at the 135° position when the electron beam is along position C in Fig. 1. A ratio of unity indicates that the product of the detector solid angle and efficiency is the same for the two detectors. The line at the value of 1.0 is for comparison only.

efficiency of the neutron detectors. In order to determine the energy dependence of the neutron detector efficiency, separate experiments were performed with the detectors held fixed and the photoneutron target replaced with a ${}^{252}\text{Cf}$ source in a fission chamber. The neutron energies are determined by measuring the time of flight between events in the fission chamber and neutron events in the plastic scintillators. The energy dependence of the efficiency curves was determined by comparing the results with the well-known⁶ fission spectrum for ${}^{252}\text{Cf}$. A typical neutron detector efficiency shape is shown in Fig. 4. The efficiency measurements were made both immediately preceding and immediately following a photoneutron experiment. Note that these neutron detector efficiency measurements include the effects of 2.0 cm thick Pb

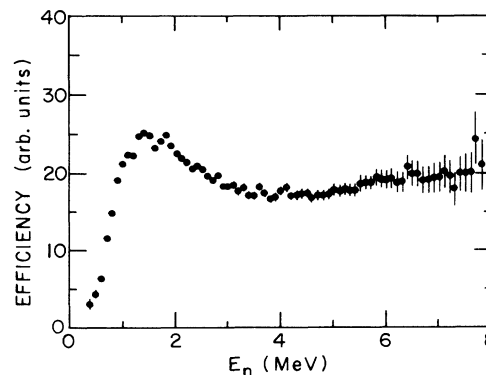


FIG. 4. Shape of the neutron detector efficiency as a function of neutron energy. This shape is determined relative to the ${}^{252}\text{Cf}$ fission spectrum.

plates which shielded the detectors from the intense γ flash of the pulsed electron accelerator and the Pb accounts for the apparent structure. The correction for the relative efficiency change is small owing to the fact that the relative kinematic shift is typically only ≤ 0.5 MeV below $E_\gamma = 10$ MeV and the fact that the photoneutron data lie above $E_n = 1.0$ MeV, where the efficiency is not strongly energy dependent. It is estimated that the error involved in this correction is $\leq 1\%$ in the ratios.

A larger correction to the data arises from neutron multiple scattering in the target. The experiment was performed at electron energies of 10.0 or 11.0 MeV and 19.0 MeV in order to minimize multiple scattering. In particular, the lower endpoint energy is expected to minimize photoneutrons produced at higher energy which can scatter down to a lower energy. However, we note that after the multiple scattering corrections are applied the high and low electron endpoint-energy experiments are in excellent agreement. As an illustration of the magnitude of the multiple scattering correction, the correction factors which were applied to the results at $E_e = 19.0$ MeV are given in Fig. 5. Of course, the corrections are largest for the high endpoint energy but do not exceed 7% in the worst case, i.e., $\theta_n = 155^\circ$ at $E_n \approx 2$ MeV. In this figure the points represent the results of a Monte Carlo neutron multiple-scattering code which was applied to the present target geometry, while the curves are spline fits to these points and the actual correction was taken from the curves. The corrections are small owing to the thin targets ($2.5 \text{ cm} \times 3.8 \text{ cm} \times 0.2$ or 0.3 cm thick) used in the present work. Previous experience with the multiple scattering code applied to thicker targets indicates that the accuracy with which the correction can be made is approximately 20%. This uncertainty would lead to a systematic error in the ratios of no more than 1.47% at 155° and $\leq 0.5\%$ at the other angles.

The largest single source of systematic error in this measurement is the determination of the reaction angle. In order to minimize this source of error the following procedure was performed. A laser was placed at the detector position and a front-surfaced mirror at the target position. The mirror was rotated until the beam reflected

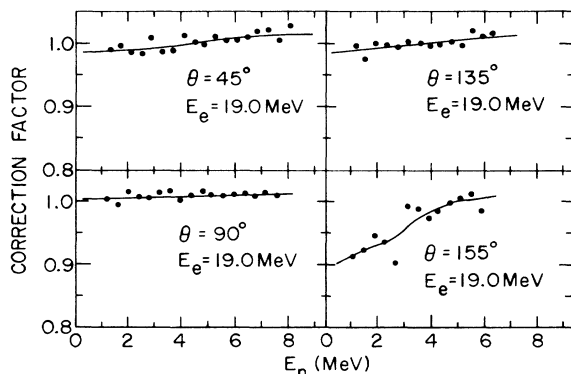


FIG. 5. The points represent correction factors for neutron multiple scattering determined from a Monte Carlo multiple scattering code. The curves represent fits to these points.

back to the laser and then rotated again until it reflected to the electron beam position. The difference in the mirror settings then allows a determination of the reaction angle. The beam position was determined by allowing the electron beam to irradiate a graduated Mylar tape during the experiment. Several tapes were irradiated during the course of each experiment in order to verify that the beam position was constant. The angular range intercepted by the detectors was approximately 0.6° and the absolute angles were determined to $\pm 0.4^\circ - 0.7^\circ$. This uncertainty in angle represents the dominant systematic error. This uncertainty in the reaction angle leads to an error in the ratios of approximately 1.3%, 2.3%, and 3.1% for the ratios at 45° , 135° , and 155° , respectively. In order to compare all the data at the same "standard" reaction angles (45° , 90° , 135° , and 155°), the calculation of Partovi⁷ was used as a guide to extrapolate the measured values to those at the standard angles. In the worst case the extrapolation spanned 3° , and, thus, the error introduced in this procedure is negligible in comparison with either the statistical or systematic errors.

III. RESULTS AND DISCUSSION

The final results are based upon eight separate photoneutron experiments excluding the solid angle checks and efficiency measurements. The results of these separate experiments are summarized in Fig. 6. These in-

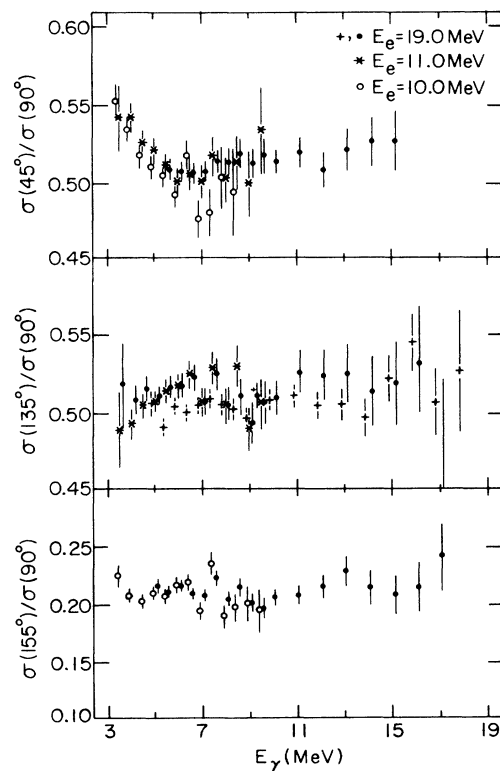


FIG. 6. Summary of all measured angular distribution ratios for the ${}^2\text{H}(\gamma, n)\text{H}$ reaction as a function of photon energy. The energies labeled E_e refer to the electron energies of the individual experiments. Statistical errors only are shown.

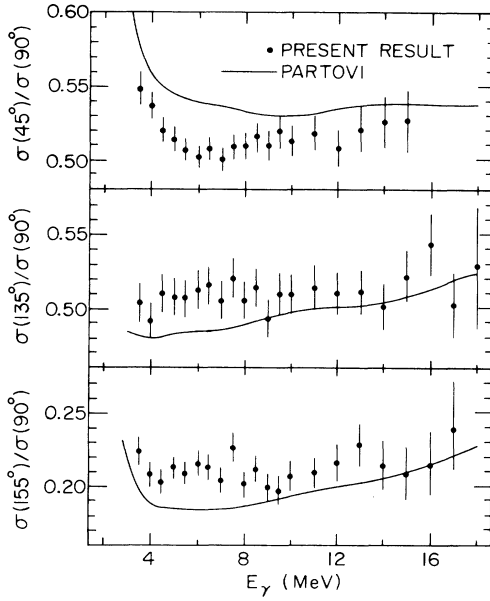


FIG. 7. Final angular distribution ratios as a function of photon energy. The systematic error has been added in quadrature with the statistical errors to produce the displayed error limits. The curves represent the predictions of Partovi. The disagreement between the theoretical calculations and the present results is significant below 10 MeV.

dividual experiments were conducted during a calendar period of approximately 6 months, whereas each experiment required only 3 d of beam time. The excellent agreement among the results is a good indication of the reproducibility of the experiment. In this figure only the statistical errors are given. It is interesting to note that there is good agreement among the high and low endpoint experiments indicating that the present discrepancy cannot be explained by a systematic difference between the low and high endpoint-energy experiments.

The results of these separate experiments were combined in order to reduce the statistical errors and the final results are shown in Fig. 7 and listed in Table I. Here, the error bars include both the statistical and systematic errors; the dominant systematic error arises from the uncertainty in the reaction angle. The curves in this figure represent the theoretical prediction of Partovi.⁷ Here, the large discrepancy between the experiment and theoretical calculation is evident below 10 MeV. The present results indicate that the theoretical calculation is shifted too far forward with respect to the data. This is a signature that the amplitudes which multiply the $\cos\theta$ terms in the Partovi expansion, given in the center-of-mass frame below, are incorrect,

$$\frac{d\sigma}{d\Omega} = a + b \sin^2\theta + c \cos\theta + d \sin^2\theta \cos\theta + e \sin^2\theta \cos^2\theta,$$

where the values $a-e$ are known as the Partovi coefficients. The terms which most likely are in error are c or

TABLE I. Final results for the measured angular distribution ratios.

E_γ (MeV)	$R_{45} =$ $\frac{\sigma(45^\circ)}{\sigma(90^\circ)}$	ΔR_{45}	$R_{135} =$ $\frac{\sigma(135^\circ)}{\sigma(90^\circ)}$	ΔR_{135}	$R_{155} =$ $\frac{\sigma(155^\circ)}{\sigma(90^\circ)}$	ΔR_{155}
3.5	0.548	0.012	0.503	0.014	0.224	0.010
4.0	0.537	0.009	0.492	0.012	0.208	0.008
4.5	0.520	0.009	0.510	0.013	0.203	0.008
5.0	0.514	0.008	0.507	0.013	0.212	0.008
5.5	0.507	0.008	0.506	0.013	0.209	0.008
6.0	0.501	0.008	0.513	0.013	0.216	0.008
6.5	0.507	0.008	0.515	0.013	0.213	0.008
7.0	0.500	0.008	0.506	0.013	0.204	0.008
7.5	0.509	0.009	0.521	0.014	0.226	0.010
8.0	0.509	0.009	0.505	0.013	0.201	0.008
8.5	0.515	0.010	0.514	0.014	0.211	0.009
9.0	0.509	0.011	0.492	0.013	0.199	0.009
9.5	0.519	0.012	0.510	0.014	0.197	0.010
10.0	0.512	0.010	0.509	0.013	0.207	0.009
11.0	0.518	0.012	0.514	0.014	0.209	0.010
12.0	0.507	0.013	0.510	0.014	0.215	0.012
13.0	0.520	0.015	0.510	0.015	0.228	0.015
14.0	0.525	0.018	0.501	0.016	0.214	0.015
15.0	0.526	0.021	0.521	0.018	0.208	0.018
16.0			0.542	0.021	0.215	0.022
17.0			0.501	0.022	0.241	0.030
18.0			0.527	0.041		

d and these coefficients depend primarily on the product of $E1$ and $E2$ amplitudes.

The present results are of unprecedented accuracy and can, in principle, place new constraints on the theoretical calculations. In particular, it is noted that if the coefficient d were 30% larger in magnitude than the present theoretical value, then the discrepancy below 10 MeV would vanish. In principle, a large value of c would also account for the present result, but the magnitude of c would have to be increased by an approximate value of 30 over the presently accepted theoretical value, i.e., c would have to be 3% the value of b to remove the present discrepancy. Although present data do not rule out this value of c , it is unlikely that the theoretical value could be changed that dramatically. Measurements at very forward or backward angles would provide a better constraint on c . Although it is difficult to understand how the $E2$ amplitudes could be in error by $\sim 30\%$, no other data overrule an increase of this magnitude. In addition, we note that neither meson-exchange current corrections nor the effect of Δ excitations have been included in the $E2$ operator to date.

The choice of the N-N potential makes little difference on the calculated angular distributions at these low photon energies. The Partovi code was modified to accept the Argonne V14 potential⁸ rather than the Hamada-Johnson potential and the results for the angular distributions were indistinguishable from one another. Thus, it is likely that the problem resides in the electromagnetic operator. Corrections to the $M1$ operator from meson-exchange currents have little influence on these angular distributions and it is unlikely that correcting the $M1$ amplitudes will play any role in resolving this discrepancy. However,

these cross section ratios are very sensitive to the presence of $E2$ transitions and it is likely that the present data are indicating a deficiency in the $E2$ amplitudes. This disagreement suggests that the discrepancy previously observed in photoneutron polarization measurements^{1,2} is not caused by the meson-exchange current correction to the $M1$ amplitudes, but rather by an inadequacy in the reaction mechanism itself.

IV. CONCLUSIONS

We have provided the highest accuracy relative angular distribution measurements available for the ${}^2\text{H}(\gamma, n)\text{H}$ reaction below 18 MeV. The results depart significantly from the accepted theoretical calculations below 10 MeV. There is a strong indication that the $E2$ excitations are not adequately described by the theoretical treatments.

ACKNOWLEDGMENTS

We wish to thank Professor E. Lomon for many useful discussions and for providing us with a copy of Dr. F. Partovi's computer code. We thank Dr. R. Wiringa for assistance with implementing the Argonne V14 potential in Partovi's code. We thank Professor E. Hadjimichael for many useful discussions. We are indebted to Dr. R. E. Holland for assistance with the data analysis. In addition, we thank Dr. A. Smith for the loan of the ${}^{252}\text{Cf}$ source and fission chamber. Finally, we thank G. Mavrogenes, D. Ficht, and L. Rawson for the design and installation of the novel electron beam transport system. This work was supported by the U. S. Department of Energy under Contract W-31-109-ENG-38.

*Present address: EMR Photoelectric Co., P.O. Box 44, Princeton, NJ 08540.

†Present address: California Institute of Technology, Pasadena, CA 91125.

¹R. J. Holt, K. Stephenson, and J. R. Specht, *Phys. Rev. Lett.* **50**, 577 (1983); M. L. Rustgi, R. Vyas, and M. Chopra, *ibid.* **50**, 236 (1983).

²J. P. Soderstrum and L. D. Knutson, *Phys. Rev. C* **35**, 1246 (1987).

³See, for example, E. G. Fuller, *Phys. Rev.* **79**, 303 (1950); R. Bösch, J. Lang, R. Müller, and W. Wölfli, *Helv. Phys. Acta*

36, 657 (1963); J. M. Cameron, *J. Phys.* **62**, 1019 (1984), and references therein.

⁴J. L. Friar, B. F. Gibson, and G. L. Payne, *Phys. Rev. C* **30**, 441 (1984); A. Cambi, B. Mosconi, and P. Ricci, *Phys. Rev. Lett.* **48**, 426 (1982).

⁵E. Hadjimichael, M. L. Rustgi, and L. N. Pandey (unpublished).

⁶P. Guenther *et al.*, Argonne National Laboratory Report No. NDM-19, 1976.

⁷F. Partovi, *Ann. Phys. (N.Y.)* **27**, 79 (1964).

⁸R. B. Wiringa *et al.*, *Phys. Rev. C* **29**, 1207 (1984).